Applied Physics Letters ARTICLE scitation.org/journal/apl

High-temperature (350 °C) oxidized iridium Schottky contacts on β-Ga_2O_3

Cite as: Appl. Phys. Lett. **114**, 233503 (2019); doi: 10.1063/1.5099126
Submitted: 7 April 2019 · Accepted: 19 May 2019 ·
Published Online: 12 June 2019

View Online Export Citation CrossMark

Caixia Hou,[1,2] Robert A. Makin,[3] Krystal R. York,[3] Steven M. Durbin,[3] Jonty I. Scott,[2,4] Rodrigo M. Gazoni,[2,4] Roger J. Reeves,[2,4] and Martin W. Allen[1,2,a)]

AFFILIATIONS

[1]Department of Electrical and Computer Engineering, University of Canterbury, Christchurch 8140, New Zealand
[2]MacDiarmid Institute for Advanced Materials and Nanotechnology, Wellington 6012, New Zealand
[3]Department of Electrical and Computer Engineering, Western Michigan University, Kalamazoo, Michigan 49008-5329, USA
[4]School of Physical and Chemical Sciences, University of Canterbury, Christchurch 8140, New Zealand

[a)]**Electronic mail:** martin.allen@canterbury.ac.nz

ABSTRACT

Oxidized iridium (IrO_x) Schottky contacts (SCs) with excellent high temperature stability were fabricated on $(\bar{2}01)$ β-Ga_2O_3 single crystal substrates. These IrO_x:β-Ga_2O_3 SCs were operated at temperatures from 24 to 350 °C with only a very small increase in reverse leakage current, while maintaining extremely high rectification ratios (at ±3 V) of more than 10 orders of magnitude at all temperatures, including 350 °C. This remarkable high temperature performance was due to their very high and thermally stable rectifying barriers that, after an initial heat-related improvement, were characterized by zero-bias effective barrier heights of 2.05 ± 0.02 eV and ideality factors of 1.05–1.10, which were almost unchanged by further repeated operation at 350 °C. The reverse leakage current density at 350 °C was only $\sim 2.3 \times 10^{-9}$ A cm^{-2} (~3.0 pA) at −3 V and $\sim 7.5 \times 10^{-8}$ A cm^{-2} (~100 pA) at −100 V. These IrO_x:β-Ga_2O_3 SCs represent a significant improvement in high-temperature β-Ga_2O_3 SC performance, with considerable potential for the fabrication of high temperature β-Ga_2O_3 rectifying diodes, deep UV photodetectors, and metal-semiconductor field effect transistors.

Beta-phase gallium oxide (β-Ga_2O_3) is a wide bandgap semiconductor that is attracting increasing interest for high-efficiency power electronic devices and deep UV photodetectors capable of undergoing high temperature operation.[1–3] Both its bandgap (E_g = 4.85 eV) and breakdown strength (~8 MV/cm) are significantly higher than those of SiC and GaN, and consequently, β-Ga_2O_3 power devices can potentially be scaled to smaller dimensions, thereby increasing their speed and efficiency.[4,5] Unlike SiC and GaN, single crystal β-Ga_2O_3 can be grown using bulk melt-growth techniques, providing a readily available source of high-quality native substrates.[6,7] The main weakness of β-Ga_2O_3 is its relatively low thermal conductivity which at ~10–30 W m^{-1} K^{-1} is an order of magnitude lower than that of SiC and GaN.[2,8] Consequently, the development of thermally stable electronic device components is critical to the widespread adoption of β-Ga_2O_3 as a viable alternative to SiC and GaN.

Schottky contacts (SCs) are key components in UV photodiodes, high-speed rectifying diodes, and metal-semiconductor field effect transistors.[9–11] In previous work, we have shown that oxidized noble metal layers consistently produce high-quality SCs in a range of oxide semiconductors, including β-Ga_2O_3.[12–15] This was attributed to the passivation of oxygen vacancies near the SC interface combined with a significant increase in the work function of the SC metal on oxidation.[16,17] In this work, we investigate the high temperature performance of oxidized iridium (IrO_x) SCs on single crystal $(\bar{2}01)$ β-Ga_2O_3 substrates. We show that IrO_x:β-Ga_2O_3 SCs have a remarkable thermal stability, capable of undergoing operation at 350 °C with very little increase in reverse leakage current and a very high rectification ratio (measured at ±3 V) of more than 10 orders of magnitude. The low reverse leakage current at 350 °C is a consequence of the very high rectifying barriers of the IrO_x:β-Ga_2O_3 SCs that were stable against repeated thermal cycling to 350 °C. This represents a significant advance in high-temperature β-Ga_2O_3 SC performance and provides a pathway to the fabrication of thermally stable β-Ga_2O_3 rectifying diodes and transistors.

The β-Ga_2O_3 material used in this work was an unintentionally doped $(\bar{2}01)$ bulk single crystal substrate ($5.0 \times 5.0 \times 0.65$ mm^3) from Tamura Corporation (Japan), grown using the edge-defined film-fed method,[7] with a resistivity, carrier density, and mobility of 0.25 Ω cm,

1.3×10^{17} cm^{-3}, and 210 cm^2 V^{-1} s^{-1}, respectively, determined by 0.51 T Hall effect measurements at 298 K. The net doping density (N_D) measured by 1 MHz capacitance-voltage measurements was 1.6×10^{17} cm^{-3} at 298 K. The as-received β-Ga_2O_3 substrate was cleaned using ultrasonically agitated acetone, methanol, and isopropyl alcohol. SCs of area 1.34×10^{-3} cm^2 were patterned onto the substrate surface using an AZ1518 photoresist and a tetramethylammonium hydroxide developer. The IrO_x SCs were deposited at room temperature (RT) via reactive sputtering of a 3-in. diameter Ir target (purity 99.95%) using an oxidizing 50 W rf plasma (13.56 MHz) established using an O_2:Ar gas mixture of 4.0:10.0 standard cubic centimeters per minute at a pressure of 4.0×10^{-3} mBar. The thickness of the resulting IrO_x layer was 35 nm, as determined by atomic force microscopy (AFM). The oxidized SCs were capped with a further 35 nm layer of plain Ir, deposited *in-situ* on top of the IrO_x layer followed by a single lift-off step. Ti/Au (50/50 nm) ohmic contacts were deposited by e-beam evaporation to complete a planar Schottky diode geometry, with a minimum separation of 30 μm between the circular SCs and L-shaped ohmic contacts, as shown in detail elsewhere.[18] The Ti/Au ohmic contacts were not annealed, but their ohmic behavior was confirmed from two probe *I-V* measurements on adjacent contacts.

The morphology of the IrO_x SC layer was investigated via AFM [Fig. 1(a)] that revealed a dense film of thickness 35 nm with a uniform grain size of 22 nm and a root mean square roughness of 0.6 nm. The composition of the IrO_x layer was measured on thicker films (~120 nm) deposited under the same reactive sputtering conditions on glassy carbon substrates using Rutherford backscattering spectrometry (RBS) and X-ray photoelectron spectroscopy (XPS) using monochromatic Al Kα 1486.6 eV X-rays and a Kratos XSAM800 spectrometer. All the XPS spectra in this work were taken from the as-deposited surface without any surface sputtering. The oxygen fraction x from RBS was 2.58 which was close to the value of x = 2.65 obtained from the XPS survey spectra, shown in Fig. 1(b). X-ray diffraction (XRD) measurements on ~120 nm thick films deposited on $(\bar{2}01)$ β-Ga_2O_3, glassy carbon, and quartz substrates [Fig. 1(c)] revealed that the IrO_x layer was amorphous (i.e., no crystalline IrO_x peaks observed on any of these substrates) and therefore can be considered to be an oxygen-rich phase with low long-range order. Figure 1(d) shows the valence band XPS spectra of the amorphous IrO_x layer that was carefully ground to the spectrometer so that the zero of the binding energy scale coincides with the Fermi level (E_F). This shows a continuous high density of states up to E_F, indicating a metalliclike nature, which was confirmed by its low resistivity of 4.93×10^{-3} Ω cm measured using annealed Ti/Au van der Pauw contacts.

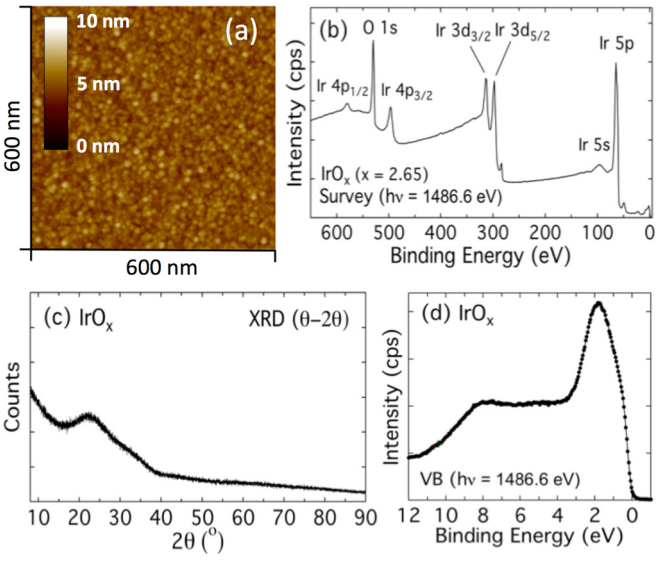

FIG. 1. (a) Atomic force microscopy image of the as-grown (uncapped) 35 nm thick IrO_x SC layer; (b) XPS survey spectrum ($h\nu = 1486.6$ eV); (c) XRD θ-2θ scan; and (d) XPS valence band spectrum ($h\nu = 1486.6$ eV) on ~120 nm thick IrO_x layers grown on glassy carbon [in (b) and (d)] and quartz [in (c)].

Figure 2(a) shows the typical current-voltage-temperature (*I-V-T* and *J-V-T*) characteristics of the IrO_x:β-Ga_2O_3 SCs measured in air and in dark conditions, from RT to 350 °C in 25 °C steps, using 150 μm diameter stainless steel probes to avoid scratching the SCs at high temperatures. The measurements were performed using a single probe on each electrode connected to a source/measure unit of a HP4155A parameter analyzer. During these measurements, the sample was bonded to a thermostatically controlled Honton HT-2008 (50×80 mm^2) heating plate, with a control accuracy of ±1 °C, using thermally conductive paste with the plate temperature checked using a Fluke Ti20 thermal imaging camera. All measurements were

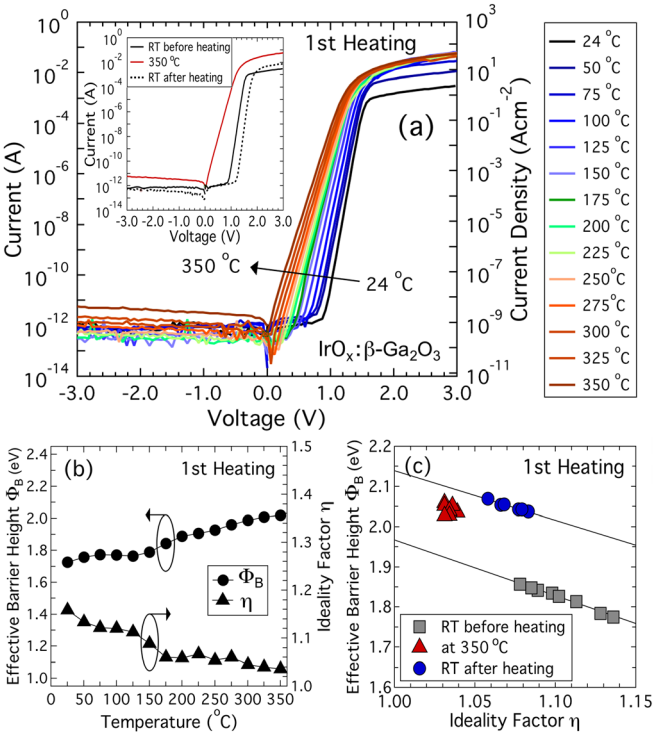

FIG. 2. (a) Typical *J-V-T* characteristics of IrO_x:β-Ga_2O_3 SCs on $(\bar{2}01)$ β-Ga_2O_3 during their first heating cycle to 350 °C; (b) zero-bias effective barrier height Φ_B and ideality factor η extracted from the *J-V-T* characteristics using thermionic emission theory; (c) Φ_B vs η plots before, during, and after the first 350 °C heating cycle and the corresponding linear fits. The inset of (a) shows the *I-V* characteristics of a typical IrO_x:β-Ga_2O_3 SC before, during, and after the first heating cycle.

performed inside a Faraday cage, resulting in a current noise floor of ~200 fA.

The *J-V-T* characteristics in Fig. 2(a) showed a constant exponential rise in forward current over many decades, consistent with thermionic emission over a single Schottky barrier. Very high rectification ratios ($J_{forward}/J_{reverse}$ at ±3 V) of more than 10 orders of magnitude were observed at all temperatures. Remarkably, only a very small increase in reverse leakage current was observed at 350 °C. The SCs were held at 350 °C for at least 30 min during which time their *J-V* characteristics remained unchanged with $J_{reverse}$ (at −3 V) remaining below 5×10^{-9} A cm^{-2} ($I_{reverse} < 6$ pA).

The forward *J-V-T* characteristics in Fig. 2(a) were analyzed using thermionic emission theory to determine the zero-bias effective barrier height (Φ_B) and the ideality factor (η) at each temperature. Using this approach, the following equation was used to fit the forward current:

$$J = J_s\left\{\exp\left[\frac{q(V - IR_s)}{\eta kT}\right] - 1\right\}, \quad (1)$$

where the saturation current density $J_s = A^*T^2 exp(-q\Phi_B/kT)$, R_s is the series resistance of the SC, and A^* is the effective Richardson constant [=41 A cm^{-2} K^{-2} for β-Ga_2O_3 assuming an effective electron mass of 0.34 m_e].[19] The ideality factor η quantifies the influence of barrier height inhomogeneities and should be close to unity for ideal laterally homogenous SCs.[20,21]

Figure 2(b) shows the evolution of Φ_B and η at each heating step from RT to 350 °C for a typical IrO_x:β-Ga_2O_3 SC. A significant increase in Φ_B with temperature, especially above 150 °C, was observed with Φ_B reaching a value of 2.04 eV at 350 °C, compared to an initial value of ~1.75 eV at RT. At the same time, η decreased from ~1.4 at RT to 1.04 at 350 °C. The increase in Φ_B and the corresponding decrease in η were permanent and remained almost unchanged after cooling back to RT. Figure 2(c) shows Φ_B vs η plots for multiple IrO_x:β-Ga_2O_3 SCs measured at (i) RT before heating, (ii) 350 °C, and (iii) RT after heating, confirming that this was a consistent effect across many devices.

To investigate the origin of the increase in Φ_B, the IrO_x SC layer from Fig. 1(a) was heated in air at 350 °C for 30 min after which no significant change in the grain size or crystallinity was observed via AFM and XRD. However, XPS survey spectra revealed an increase in oxygen fraction x from 2.65 to 3.66. The oxidation of noble metals is known to increase their work function, and therefore, an increase in the oxidation of the IrO_x:β-Ga_2O_3 SCs on heating could explain their increased Φ_B,[22] although a more detailed investigation including the effect of the Ir capping layer on SC oxidation would be needed to confirm this.

It is also possible that a heat-related improvement in the Ti/Au ohmic contacts may have occurred. Since these showed well-behaved ohmic behavior (i.e., linear *I-V* characteristics) before and after the first 350 °C heating cycle, any such improvement would not affect the increase in Φ_B of the IrO_x:β-Ga_2O_3 SCs but could cause a decrease in R_s. A comparison of the RT *I-V* characteristics of the SCs before and after the first heating cycle [Fig. 2(a) inset] revealed an increase in forward current at V > +2.5 V, which is consistent with a lower R_s due to a decrease in Ti/Au contact resistance.

Following this initial heat-related improvement in Φ_B, the *J-V-T* characteristics of the IrO_x:β-Ga_2O_3 SCs were re-measured, with the results shown in Fig. 3(a). During this second 350 °C heating cycle, the SCs again showed well-behaved single-exponential thermionic

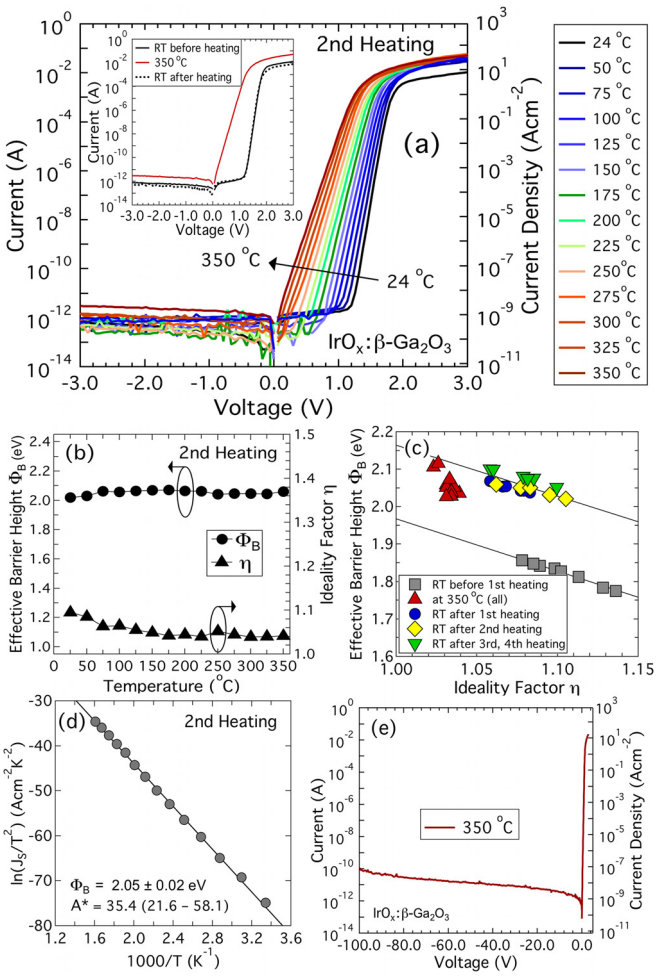

FIG. 3. (a) Typical *J-V-T* characteristics of IrO_x:β-Ga_2O_3 SCs on $(\bar{2}01)$ β-Ga_2O_3 during their second heating cycle to 350 °C; (b) Φ_B and η extracted from the *J-V-T* characteristics; (c) Φ_B vs η plots during and after various 350 °C heating cycles; (d) Richardson plot for a typical IrO_x:β-Ga_2O_3 SC with a least-squares fit from which Φ_B and A* were determined; (e) typical *J-V-T* characteristics at reverse biases of 0 to −100 V. The inset in Fig. 3(a) shows the *I-V* characteristics of a typical IrO_x:β-Ga_2O_3 SC before, during, and after the 2nd heating cycle.

emission under forward bias, with only a very small increase in reverse-bias leakage current [$J_{reverse}$ (at −3 V) = 2.3×10^{-9} A cm^{-2} (3.0 pA) at 350 °C] and with rectification ratios (at ±3 V) again in excess of 10^{10} at all temperatures. In contrast to the first heating cycle, Φ_B remained almost constant at the initial RT value of 2.04 eV with a much smaller decrease in η with temperature. Several further heating cycles to 350 °C also resulted in very similar *J-V-T* characteristics with no further significant changes in Φ_B, as shown in the Φ_B vs η plots for multiple SCs in Fig. 3(c). This confirms that, after an initial improvement, the rectifying barriers of the IrO_x:β-Ga_2O_3 SCs were thermally stable, at least up to 350 °C. Interestingly, a further small improvement in Φ_B to ~2.10 eV was observed after the 3rd and 4th heating cycles to 350 °C, suggesting that any long term changes in Φ_B are likely to be in the direction of increasing Φ_B. The lack of significant variation in $J_{reverse}$ at temperatures below 350 °C is also interesting. This may be

partly due to the fact that the β-Ga_2O_3 surface between the Schottky and ohmic contacts was bare and unpassivated, which may introduce a shunt resistance in parallel to the rectifying barrier.

The *J-V-T* characteristics in Fig. 3(a) were also used to construct a Richardson plot, shown in Fig. 3(d), from which values of Φ_B and A^* were determined from a linear least-squares fit to the data using the relationship $\ln(J_s/T^2) = \ln(A^*) - q\Phi_B/kT$. The resulting value of $\Phi_B = 2.05 \pm 0.02$ eV was close to the individual values shown in Fig. 3(b), while the value of $A^* = 35.4$ A cm^{-2} K^{-2} was close to the theoretical value of 41.0 A cm^{-2} K^{-2} within the uncertainty of (21.6–58.2) A cm^{-2} K^{-2} arising from the extrapolation of the linear fit in Fig. 3(d) to 1000/kT = 0. Figure 3(e) shows the reverse *J-V-T* characteristics at 350 °C over an extended reverse bias range up to −100 V for a typical IrO_x:β-Ga_2O_3 SC. The reverse current density was less than 8.0×10^{-8} A cm^{-2} (~100 pA) at −100 V with Φ_B and η unchanged after this stress test. In terms of breakdown voltage, some of the IrO_x:β-Ga_2O_3 SCs tested showed the beginning of soft break down at approximately −90 V although several devices including that shown in Fig. 3(e) could withstand reverse biases of −100 V despite their simple geometry.

In addition to these *J-V-T* measurements, capacitance-voltage-temperature *C-V-T* measurements were taken at a frequency of 1 MHz using a Boonton 7200 Precision Capacitance Meter over the same temperature range. The capacitance of a SC under an applied bias *V* is given by

$$\frac{A^2}{C^2} = \left(\frac{2}{\varepsilon_s \varepsilon_0 q N_D}\right)\left(V_{bi} - \frac{kT}{q} - V\right), \tag{2}$$

where ε_s is the static dielectric constant (=10 for β-Ga_2O_3),[2] ε_0 the permittivity of free space, N_D the net donor density of the β-Ga_2O_3 substrate, and V_{bi} the built-in voltage of the SC. The barrier height (from *C-V* measurements) can be determined using $\Phi_{B,CV} = qV_{bi} + \xi$, where $\xi = (kT/q)\ln(N_C/N_D)$ is the energetic separation between the Fermi level and the conduction band minimum and $N_C = 2(2\pi m_e^* kT/h^2)^{3/2}$ is the conduction band effective density of states which was calculated at each temperature assuming an effective electron mass of $0.34 \cdot m_e$.[2]

Figure 4(a) shows plots of A^2/C^2 vs V from RT to 350 °C for a typical IrO_x:β-Ga_2O_3 SC. The extracted values of $\Phi_{B,CV}$ and N_D are shown in Fig. 4(b), with $\Phi_{B,CV}$ showing a slight decrease from 2.18 eV (RT) to 2.08 eV (350 °C), while N_D increased from 1.60×10^{17} to 1.83×10^{17} cm^{-3} over the same temperature range. The changes in $\Phi_{B,CV}$ and N_D were fully reversible after cooling to RT and were also reproduced in several other IrO_x:β-Ga_2O_3 SCs matching the thermal stability in Φ_B observed in the *J-V-T* characteristics. A slight decrease in $\Phi_{B,CV}$ was also observed by Higashiwaki *et al.*[19] in Pt/(001)β-Ga_2O_3 SCs over the temperature range of 21–200 °C although the underlying cause was not completely certain.

Figure 4(b) also shows the image-force-corrected barrier height $\Phi_{B,IF}$ at each temperature. These are the values of Φ_B from the corresponding *J-V-T* measurements corrected for the image force effect that lowers the barrier height by[20,21]

$$\Delta\Phi_{if} = \left[\left(\frac{q^3 N_D}{8\pi^2 \varepsilon_\infty^2 \varepsilon_s \varepsilon_0^3}\right)\left(\Phi_B - \xi - \frac{kT}{q}\right)\right]^{1/4}, \tag{3}$$

where ε_∞ is the optical dielectric constant, which is taken to be 3.5 for β-Ga_2O_3.[2] The values of Φ_B determined by *J-V* and *C-V* measurements, shown in Fig. 4(b), are in reasonable agreement, indicating that any lateral inhomogeneity in the IrO_x:β-Ga_2O_3 SCs is also reasonably low, as would also be expected from their close-to-unity ideality factors.[23]

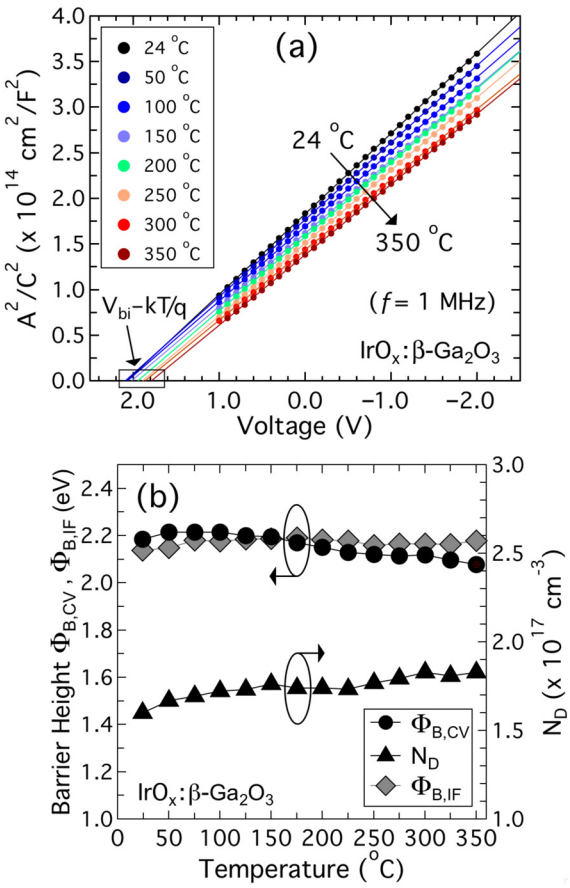

FIG. 4. (a) Typical *C-V-T* characteristics of IrO_x:β-Ga_2O_3 SCs on $(\bar{2}01)$ β-Ga_2O_3 during the third heating cycle to 350 °C including the linear least-squares fits used to extract $V_{bi} - kT/q$ (y = 0 intercept) and N_D (inverse slope); (b) barrier height $\Phi_{B,CV}$ and N_D over the range of 24–350 °C determined from the *C-V-T* measurements and the image-force-corrected barrier height $\Phi_{B,IF}$ from the corresponding *J-V-T* measurements.

There are relatively few reports of β-Ga_2O_3 SC operation above 200 °C in the literature: Higashiwaki *et al.*[19] characterized the performance of Pt SCs on β-Ga_2O_3 layers grown by halide vapor phase epitaxy from 21 to 200 °C with $\Phi_B = 1.15$ eV (21 °C) and 1.09 eV (200 °C) and with a saturation current density of ~10^{-5} A cm^{-2} at 200 °C. Tadjer *et al.*[24] measured the 30–210 °C *J-V-T* characteristics of TiN and Pt SCs on $(\bar{2}01)$ β-Ga_2O_3 single crystal substrates ($n \sim 3 \times 10^{17}$ cm^{-3}) with $\Phi_B = 1.01$ and 0.98 eV, respectively, at RT. At 210 °C, the reverse leakage current densities (at −3.0 V) were greater than 10^{-5} and 10^{-2} A cm^{-2} for the Pt and TiN SCs, respectively, with rectification ratios (at ±0.6 V) of less than 10^5 and 10^4, respectively. Most recently, Fares *et al.*[25] investigated the high-temperature performance of W/Au and Ni/Au SCs on $(\bar{2}01)$ β-Ga_2O_3 single crystal substrates ($n = 2 \times 10^{17}$ cm^{-3}) with $\Phi_B = 0.97$ and 1.21 eV at RT,

respectively, although both of these decreased on heating. The rectification ratios (compared at +2.0 V/−1.0 V) of the W/Au and Ni/Au SCs were $\sim 10^4$ and $\sim 10^6$ at 300 °C and $\sim 10^2$ and $\sim 10^4$ at 400 °C, respectively. The corresponding 300 °C reverse leakage current densities at −1.0 V were $\sim 10^{-2}$ and $\sim 10^{-4}$ A cm^{-2}, respectively. The high-temperature rectifying performance of the IrO_x:β-Ga_2O_3 SCs in this work, with rectification ratios (at ±3.0 V) of more than 10^{10} at 350 °C and the very small increase in reverse leakage current at 350 °C to less than 2.5×10^{-9} A cm^{-2} (∼3 pA) at −3.0 V and less than 8.0×10^{-8} A cm^{-2} (∼100 pA) at −100 V, represents a significant improvement in the thermal stability of β-Ga_2O_3 SCs. This is a direct consequence of their very large ($\Phi_B > 2.0$ eV) and thermally stable rectifying barriers that restrict the magnitude of the reverse leakage current even at high temperatures.

In conclusion, reactively rf-sputtered oxidized iridium (IrO_x) SCs on $(\bar{2}01)$ β-Ga_2O_3 showed excellent thermal stability up to 350 °C. After an initial and permanent increase in Φ_B from ∼1.75 to 2.05 ± 0.02 eV during the first 350 °C heating cycle, the rectifying barriers of these IrO_x:β-Ga_2O_3 SCs were remarkably stable, both during and after repeated operation at 350 °C. More than 10 orders of magnitude of current rectification (at ±3.0 V) was reproducibly observed at all temperatures up to and including 350 °C, with reverse current densities at 350 °C of less than 2.5×10^{-9} A cm^{-2} (∼3 pA) at −3.0 V and less than 8.0×10^{-8} A cm^{-2} (∼100 pA) at −100 V. These highly rectifying thermally stable SCs offer considerable potential for the future fabrication of high-temperature β-Ga_2O_3 electronic devices.

REFERENCES

[1]M. Higashiwaki and G. H. Jessen, Appl. Phys. Lett. **112**, 060401 (2018).
[2]S. J. Pearton, J. Yang, P. H. Cary, F. Ren, J. Kim, M. J. Tadjer, and M. A. Mastro, Appl. Phys. Rev. **5**, 011301 (2018).
[3]S. J. Pearton, F. Ren, M. Tadjer, and J. Kim, J. Appl. Phys. **124**, 220901 (2018).
[4]M. Higashiwaki, K. Sasaki, H. Murakami, Y. Kumagai, A. Koukitu, A. Kuramata, T. Masui, and S. Yamakoshi, Semicond. Sci. Technol. **31**, 034001 (2016).
[5]A. J. Green, K. D. Chabak, E. R. Heller, S. Member, R. C. Fitch, M. Baldini, A. Fiedler, K. Irmscher, G. Wagner, Z. Galazka, S. E. Tetlak, A. Crespo, K. Leedy, and G. H. Jessen, IEEE Electron Device Lett. **37**, 902 (2016).
[6]Z. Galazka, K. Irmscher, R. Uecker, R. Bertram, M. Pietsch, A. Kwasniewski, M. Naumann, T. Schulz, R. Schewski, D. Klimm, and M. Bickermann, J. Cryst. Growth **404**, 184 (2014).
[7]A. Kuramata, K. Koshi, S. Watanabe, Y. Yamaoka, T. Masui, and S. Yamakoshi, Jpn. J. Appl. Phys. Part 1 **55**, 1202A2 (2016).
[8]Z. Guo, A. Verma, X. Wu, F. Sun, A. Hickman, T. Masui, A. Kuramata, M. Higashiwaki, D. Jena, and T. Luo, Appl. Phys. Lett. **106**, 111909 (2015).
[9]T. Oshima, T. Okuno, N. Arai, N. Suzuki, S. Ohira, and S. Fujita, Appl. Phys. Express **1**, 011202 (2008).
[10]Z. Hu, H. Zhou, Q. Feng, J. Zhang, C. Zhang, K. Dang, Y. Cai, Z. Feng, Y. Gao, X. Kang, and Y. Hao, IEEE Electron Device Lett. **39**, 1564 (2018).
[11]M. Higashiwaki, K. Sasaki, A. Kuramata, T. Masui, and S. Yamakoshi, Appl. Phys. Lett. **100**, 013504 (2012).
[12]M. W. Allen, R. J. Mendelsberg, R. J. Reeves, and S. M. Durbin, Appl. Phys. Lett. **94**, 103508 (2009).
[13]G. T. Dang, T. Uchida, T. Kawaharamura, M. Furuta, A. R. Hyndman, R. Martinez, S. Fujita, R. J. Reeves, and M. W. Allen, Appl. Phys. Express **9**, 041101 (2016).
[14]C. Hou, R. M. Gazoni, R. J. Reeves, and M. W. Allen, Appl. Phys. Lett. **114**, 033502 (2019).
[15]C. Hou, R. M. Gazoni, R. J. Reeves, and M. W. Allen, IEEE Electron Device Lett. **40**, 337 (2019).
[16]M. W. Allen and S. M. Durbin, Appl. Phys. Lett. **92**, 122110 (2008).
[17]A. M. Hyland, R. A. Makin, S. M. Durbin, and M. W. Allen, J. Appl. Phys. **121**, 024501 (2017).
[18]A. M. Hyland, R. J. Reeves, R. A. Makin, S. M. Durbin, and M. W. Allen, J. Mater. Sci. Semicond. Process. **69**, 9 (2017).
[19]M. Higashiwaki, K. Konishi, K. Sasaki, K. Goto, K. Nomura, Q. T. Thieu, R. Togashi, H. Murakami, Y. Kumagai, B. Monemar, A. Koukitu, A. Kuramata, and S. Yamakoshi, Appl. Phys. Lett. **108**, 133503 (2016).
[20]W. Mönch, J. Vac. Sci. Technol., B **17**, 1867 (1999).
[21]W. Mönch, *Electronic Properties of Semiconductor Interfaces* (Springer-Verlag, Berlin, Germany, 2004).
[22]H. Zhang, A. Soon, B. Delley, and C. Stampfl, Phys. Rev. B **78**, 045436 (2008).
[23]J. H. Werner and H. H. Güttler, J. Appl. Phys. **69**, 1522 (1991).
[24]M. J. Tadjer, V. D. Wheeler, D. I. Shahin, C. R. Eddy, and F. J. Kub, ECS J. Solid State Sci. Technol. **6**, P165 (2017).
[25]C. Fares, F. Ren, and S. J. Pearton, ECS J. Solid State Sci. Technol. **8**, Q3007 (2019).